Author Manuscript
Author Manuscript
Author Manuscript
Author Manuscript

HHS Public Access
Author manuscript
Methods Enzymol. Author manuscript; available in PMC 2018 February 20.

Published in final edited form as:
Methods Enzymol. 2017 ; 589: 171–190. doi:10.1016/bs.mie.2017.01.011.

Probing Cdc42 polarization dynamics in budding yeast using a biosensor

Satoshi Okada[1,3,*], **Mid Eum Lee**[2,4,*], **Erfei Bi**[1,#], and **Hay-Oak Park**[2,#]

[1]Department of Cell and Developmental Biology, University of Pennsylvania Perelman School of Medicine, Philadelphia, PA 19104, USA

[2]Department of Molecular Genetics, The Ohio State University, Columbus, OH43210, USA

[3]Department of Medical Biochemistry, Kyushu University Graduate School of Medical Sciences, Fukuoka 812-8582, Japan

Abstract

Cdc42 is a small guanosine triphosphatase (GTPase) that plays a central role in polarity development in diverse cell types. Since the activity of Cdc42 is dynamically controlled in time and space, it is required to develop a biosensor to monitor its activation *in vivo*. In this chapter, we describe the construction and usage of a simple and robust biosensor for monitoring active Cdc42 in budding yeast. This affinity-based biosensor uses a red fluorescent protein fused to a Cdc42- and Rac-interactive binding (CRIB) motif from one of the Cdc42 effector proteins. Because it binds specifically to the GTP-bound Cdc42, this biosensor can be used to monitor Cdc42 activation *in vivo*. This or similar biosensors can be widely used for studying GTPase signaling in other cell types because of the conserved CRIB motif present among GTPase targets.

Keywords

Cdc42; GTPase; CRIB; FRAP; GEF; GFP

1. INTRODUCTION

Cdc42 is a highly conserved small GTPase that plays a key role in polarity development in species ranging from yeast to human (Etienne-Manneville 2004; Park & Bi 2007). In response to either internal or external cues, Cdc42 cycles between the GDP- and GTP-bound states, and its activity is dynamically controlled in time and space to enable distinct polarization events, including cytoskeletal assembly and membrane trafficking. Since Cdc42 is activated transiently at a specific region, a robust and reliable biosensor for its activation is required to probe the dynamics of Cdc42 activation in live cells.

[#]Corresponding authors: Erfei Bi, ebi@mail.med.upenn.edu; Hay-Oak Park, park.294@osu.edu.
[4]Present address: Department of Biochemistry and Cell Biology, The Geisel School of Medicine at Dartmouth, Hanover, NH 03755, USA
[*]These authors contributed equally to this work.

Author Manuscript Author Manuscript Author Manuscript Author Manuscript

Earlier use of fluorescence-based biosensors had allowed the determination of the spatio-temporal profile of GTPases' activity, providing mechanistic insights into cell polarization in different model systems. The activation patterns of multiple GTPases have been monitored by several biosensors for more than 10 years. Initially, activation of the endogenous Cdc42 had been monitored using a Wiskott–Aldrich Syndrome protein (WASP) domain that binds only to the active Cdc42. This Cdc42 effector domain labeled with a solvent-sensitive dye produced strong fluorescence signal upon its binding to the activated Cdc42 by placing the dye in a hydrophobic pocket formed by amino acids from both WASP and Cdc42 (Nalbant, Hodgson, Kraynov, Toutchkine & Hahn 2004).

Recent polarization studies involved the use of both single and dual chain fluorescence resonance energy transfer (FRET)-based biosensors for small GTPases. The intramolecular FRET-based sensor was designed for monitoring RhoA activation using a fusion construct expressing the Rho effector rhotekin (RBD, aa7–89) tagged with a cyan fluorescent protein (CFP), a variant of yellow fluorescent protein (YFP), and the full-length RhoA (Pertz, Hodgson, Klemke & Hahn 2006). Upon activation, RBD binds to Rho-GTP, which results in changes in the relative position of the two fluorophores, increasing the FRET signal. In budding yeast, a FRET-based biosensor for active Cdc42 consisted of the Cdc42/Rac-interactive binding (CRIB) domain from Cla4, a Cdc42 effector, and Cdc42 that are sandwiched by two fluorophores, GFP and mCherry (Smith, Rubinstein, Mendes Pinto, Slaughter, Unruh & Li 2013).

In this chapter, we describe the construction and usage of a simple and robust biosensor for monitoring active Cdc42 in the budding yeast *Saccharomyces cerevisiae*. The Cdc42 effector Gic2 contains a conserved CRIB motif, also known as PBD (p21-binding domain), which binds specifically to Cdc42-GTP, and localizes to the sites of polarized growth in a Cdc42-dependent manner (Jaquenoud & Peter 2000). A fragment of $Gic2^{1–208}$ containing the PBD has been tagged with fluorescent molecules and used for monitoring Cdc42-GTP in live cells (Ozbudak, Becskei & van Oudenaarden 2005; Tong, Gao, Howell, Bose, Lew & Bi 2007; Lo, Lee, Narayan, Chou & Park 2013; Okada, Leda, Hanna, Savage, Bi & Goryachev 2013; Kang, Lee & Park 2014; Lee, Lo, Miller, Chou & Park 2015). By using this affinity-based biosensor, we can monitor dynamics of Cdc42 activation in specific processes *in vivo*. This and similar biosensors of GTPases will undoubtedly play key roles in understanding the functions, mechanisms, and spatiotemporal regulation of G protein signaling in diverse cell types.

2. GENERATION OF A BIOSENSOR OF ACTIVE CDC42

2.1. Development of a Cdc42-GTP biosensor

The Cdc42 effector Gic2 contains a p21-binding domain (PBD, aa133–166) and a Cdc42/Rac-interactive binding (CRIB) domain (aa134–147) (Fig. 1a), which are required for its interaction with Cdc42-GTP. Jaquenoud and Peter reported that Gic2 localized to the sites of polarized cell growth where Cdc42-GTP was presumably concentrated, and this localization depended on its CRIB domain (Jaquenoud & Peter 2000). Based on these observations, we developed a Cdc42-GTP biosensor, Gic2-PBD-RFP, by simply fusing the N-terminal portion (aa1–208) of Gic2 to the red fluorescent protein tdTomato (Fig. 1b). As expected, an *in vitro*

Author Manuscript Author Manuscript Author Manuscript Author Manuscript

interaction assay confirmed that Gic2-PBD–RFP interacted specifically with GTP-bound Cdc42 (Fig. 1c). Gic2-PBD-RFP localized to the sites of polarized cell growth, including the presumptive bud site and bud cortex, but not the bud neck at the onset of cytokinesis (Figs. 2–5)(Ozbudak et al. 2005; Tong, Gao, Howell, Bose, Lew & Bi 2007; Lo et al. 2013; Okada et al. 2013; Kang et al. 2014; Lee et al. 2015).

To test whether Gic2-PBD-RFP signal genuinely reflected Cdc42 activity (*i.e.* the level of Cdc42-GTP) in live cells, we examined the fluorescence intensity and distribution of Gic2-PBD-RFP in *cdc24-4* mutant cells, which harbor a temperature-sensitive mutation in *CDC24* that encodes the essential GEF (guanine nucleotide exchange factor) for Cdc42 in budding yeast (Tong et al. 2007; Kang et al. 2014). When the *cdc24-4* mutant cells were cultured at the permissive temperature (25°C), Gic2-PBD-RFP signal localized at the growth sites. After a 20-minute treatment at the non-permissive temperature (37°C), the signal of Gic2-PBD-RFP disappeared from the growth sites. In wild-type cells, the Gic2-PBD-RFP signal remained at the growth sites under the same condition. This result suggested that the loss of Cdc42 GEF (Cdc24) function led to a decrease in Cdc42-GTP (or increase of Cdc42-GDP), which was followed by the loss of Gic2-PBD-RFP signal from the growth sites. Interestingly, a significant percentage of *cdc24-4* cells carrying a multi-copy *BUD3* plasmid exhibited the Gic2-PBD-RFP cluster when arrested as unbudded cells at 37°C. This observation led to the discovery of the second Cdc42 GEF Bud3 (Kang et al. 2014)(see below, 4-1). These studies demonstrated the feasibility of Gic2-PBD-RFP as a Cdc42-GTP biosensor with a sensitivity and responsiveness applicable to experiments involving live cells.

2.2. Further characterization of the Cdc42 biosensor by FRAP

We performed fluorescence recovery after photo-bleaching (FRAP) analysis (see below for the procedure) to further characterize the Cdc42-GTP biosensor *in vivo*. When the polar cap of PBD-RFP in unbudded cells was bleached, it recovered within 10 sec (Fig. 2a), although slightly more slowly than the Gic2-PBD-GFP probe, which was reported to recover its initial intensity in less than 1 sec (Ozbudak et al. 2005). Using a 0.83× 0.83 μm bleach spot, we found that Gic2-PBD-RFP recovered significantly faster with a recovery half-time of 11.8±4.5 s (Fig. 2b) compared to the GFP-fusion of GTP-locked $Cdc42^{Q61L}$, albeit somewhat slower than GFP-Cdc42 (Wedlich-Soldner, Wai, Schmidt & Li 2004; Bendezu, Vincenzetti, Vavylonis, Wyss, Vogel & Martin 2015). These data suggest that our biosensor has the specificity and dynamics for monitoring Cdc42 activity *in vivo*.

3. DETECTION AND QUANTIFICATION OF CDC42 ACTIVATION *IN VIVO*

Using the Gic2-PBD-RFP biosensor, we have monitored Cdc42 polarization dynamics throughout the cell cycle. Here we describe the standard protocols for sample preparation and the equipment used for FRAP and time-lapse imaging at University of Pennsylvania (Penn) and the Ohio State University (OSU).

Author Manuscript Author Manuscript Author Manuscript Author Manuscript

3.1 Devices

Devices used for time-lapse imaging (performed at the CDB Microscopy Core at PENN)

- Microscope: an inverted microscope (IX71; Olympus)
- Objective lens: a 100×, 1.4 NA, Plan S-Apo oil immersion (Olympus)
- Camera: a back-thinned electron multiplying CCD camera (ImagEM, C9100-13; Hamamatsu Photonics)
- Light source: diode lasers (488 nm for GFP and 561 nm for RFP) set in a laser integrator (Spectral Applied Research)
- Confocal unit: a spinning-disk confocal scan head (CSU10; Yokogawa)
- Environmental chamber: culture dish heater (DH-35; Warner Instruments)
- Control software: MetaMorph 7.7 (Molecular Devices)

Devices used for FRAP (performed at OSU)

- Microscope: an inverted microscope (Eclipse TE2000-U; Nikon)
- Objective lens: a 100×/1.4 NA Plan Apo oil immersion (Nikon)
- Light source: a 488-nm argon ion laser and 568-nm solid state laser
- Camera: a cooled charge-coupled device camera (ORCA-AG, Hamamatsu)
- Confocal system: spinning disk confocal microscope (UltraView ERS, Perkin Elmer Life and Analytical Sciences)

Devices used for time-lapse imaging (performed at OSU)

- Microscope: an inverted microscope (Ti-E; Nikon)
- Objective lens: a 100×, 1.4 NA Plan Apo oil immersion (Nikon)
- Light source: 440-, 488-, 515-, and 561-nm solid-state lasers (Modular Laser System 2.0; PerkinElmer)
- Camera: a back-thinned electron-multiplying charge-coupled device camera (ImagEM C9100-13; Hamamatsu Photonics)
- Confocal system: spinning-disk confocal microscope (Ultra-VIEW VoX CSUX1 system; PerkinElmer)
- Climate chamber: stage top incubator INUB-PPZI2-F1 equipped with UNIV2-D35 dish holder (Tokai Hit)

3.2 Sample preparation

For imaging studies at Penn

1. Inoculate yeast cells in an appropriate medium and continue to culture overnight at 25°C.

Author Manuscript Author Manuscript Author Manuscript Author Manuscript

Note: Synthetic complete (SC) medium containing 2% dextrose without buffering material is preferable because the solidity of agarose (used in later steps) will be affected by the pH of the medium. When the fluorescence intensity of the target molecules is expected to be relatively low, it is better to use yeast nitrogen base without riboflavin to reduce the background fluorescence signal from the medium.

2. Dilute the cells into fresh medium (5 - to 20-fold dilution) and continue to culture at 25°C until the cells enter the exponential growth phase (OD_{600} = 0.4–0.8).

3. Prepare culture medium containing 1.2% low-melting-point agarose and boil the medium for 10 minutes and keep the melted culture medium in a liquid form at 37°C.

4. Put the yeast liquid culture (500–700 μL) on a poly-lysine-coated glass-bottom 35-mm dish (P35GC-1.5-14.C, MatTek).

5. To settle down the yeast cells to the glass surface, incubate the sample for ~ 10 minutes.

6. Using a P1000 micropipette, aspirate the excessive supernatant gently (500–550 μL).

7. Put 1300 μL of the melted culture medium (prepared in step 3) and mix the yeast cells and the agarose-containing medium gently with a P1000 micropipette three times.

8. Incubate the dish at room temperature (~25°C) for 15 minutes to solidify the agarose layer.

9. Put 500–550 μL of liquid medium over the solidified agarose layer.

10. Incubate the sample dish at room temperature (~25°C) for 5–15 minutes to let the liquid and solid layers reach equilibrium.

11. Set the sample dish into an environmental chamber to maintain a constant condition during time-lapse imaging.

For imaging studies at OSU

Cell growth

1. Grow yeast cells overnight in synthetic media containing appropriate nutrients at 30°C. Since our imaging typically involves fluorescent proteins expressed from their endogenous chromosomal loci, we use synthetic complete (SC) containing 2% (w/v) dextrose.

2. Dilute overnight culture about 5- 10-fold in the same fresh media and grow for 4–5 hrs (to reach OD_{600} = 0.4–0.8) at 30°C prior to imaging.

Author Manuscript Author Manuscript Author Manuscript Author Manuscript

Mounting cells: For both time-lapse imaging and FRAP experiments, cells are mounted on agar pads on the glass slide as described in the following steps. Alternatively, cells can be immobilized in glass bottom dishes (see below).

1. Dissolve 2% low-melting agarose containing media (same media used for growing cells) in a microfuge tube using a heating block.
2. Clean a glass slide with a kimwipe and then attach two strips of scotch tape on both ends of the glass slide.
3. Place the slide on a cold metal block (covered with a kimwipe on the top) and drop 30 μL of the agarose mix onto the slide.
4. Place a second slide on the top of the agar mix and then flatten the agar pad by pressing evenly using the thumbs or by putting some weight (for example, placing a glass bottle containing ~50 grams of H_2O) on the top.
5. Push apart the two slides using a constant, gentle sliding action. To get a flat agar surface, it is better to detach slides while moisture still remains in the agar pad.
6. Drop ~3 μL of cell culture (spin down cells to concentrate before loading) onto the agarose pad.
7. Place a cover glass on top of the agar pad and seal the cover glass by applying nail polish or 100% pure petroleum jelly (e.g., Vaseline).

Wait a couple of minutes for the sealing to harden before using the slide for imaging.

Yeast cells can be immobilized in glass bottom dishes (35 mm; MatTek), pretreated with concanavalin A (conA; Type IV, Sigma). *Notes: Con A is a lectin that binds to carbohydrate on the yeast cell surface. ConA stock is prepared in water at 0.5 mg/ml and stored up to a year at −20°C. Alternatively, poly-lysine-coated glass-bottom dishes can be used. Mounting cells in the dish often improves the spatial resolution of a ring structure at the mother-bud neck (such as the septin ring) by positioning yeast cells vertically (i.e., the mother-bud axis is parallel to the direction of capturing Z-stacks)(Lee et al. 2015).*

1. Apply 10 μL of ConA solution into a dish and spread it with the side of a pipet tip, and air dry for about 20 min in a box to prevent dust.
2. Rinse the dish twice with water.
3. Place 100 μL of cell suspension and incubate for 20 min.
4. Wash three times with synthetic complete medium to remove cells that are not stuck to the glass bottom.
5. Place a thin layer of 0.6% agarose containing media (cooled down after melting).
6. For long-term imaging, place 500μL of liquid medium over the solidified agarose layer.

Author Manuscript Author Manuscript Author Manuscript Author Manuscript

3.3 Imaging methods

Time-lapse microscopy

1. Set the 35-mm dish sample into an environmental chamber (DH-35, Warner Instruments) mounted on the sample stage of the inverted microscope.
2. Wait for ~10 minutes until the sample temperature is stabilized.

   Note: For imaging of temperature-sensitive mutants such as cdc24-4, cells are grown overnight at room temperature, diluted to prewarmed media (37°C), and shaken for 2 hours at 37°C before imaging in a temperature-controlled environmental chamber at 37°C.
3. Use a 100× objective lens with oil immersion. When higher spatial resolution is required, it is preferable to use an objective lens with a higher numerical aperture (NA).
4. After the sample temperature is stabilized in the environmental chamber, adjust the focus to the position near the equatorial plane of the cells attached to the glass surface. If the microscope is equipped with an autofocus system, set the focal plane as a reference position at this time.

   Note: When a long time-lapse image acquisition is performed, the effect of focal drift is not negligible. If the microscope system is not equipped with an autofocus system, it is required to re-adjust the focus whenever needed, usually every 5 minutes, depending on the time interval settings and the temperature. When a higher temperature is used, the effect of focal drift is larger in general.
5. Set the parameters for image acquisition.

The duration of imaging depends on the cellular process to be monitored. If a whole cell cycle needs to be covered, 120–180-minute duration is required at 25°C. In our laboratory, 120-minute duration time is set typically.

The interval of image acquisition also depends on the speed of the target process. When Cdc42 activity is monitored, a 1–2-minute interval is typically selected.

Z-stack setting: as Cdc42 molecules can be distributed on the whole cell surface, enough Z sections must be collected to cover the entire cell to yield meaningful data. Typically, 0.6 μm × 11 z-slices (6-μm thickness in total) and 0.7 μm × 11 z-slices (7-μm thickness in total) are used for haploid and diploid strains, respectively. If an abnormally shaped and/or sized strain is monitored, appropriate Z-stack setting is required to accommodate its morphological change.

Exposure settings: to reduce the photobleaching of fluorescent proteins and to minimize the phototoxicity of the excitation light to the cells, it is essential to choose an appropriate exposure time. In general, it is better to use the shortest exposure time that provides acceptable signal-to-noise ratio. For the Gic2-PBD-RFP biosensor, 100–200 msec exposure time is used for an EMCCD camera (ImagEM, Hamamatsu photonics) with on-chip gain of 300 and no binning.

Author Manuscript Author Manuscript Author Manuscript Author Manuscript

6. Start time-lapse microscopy using appropriate imaging software such as MetaMorph to control the microscope and camera.

FRAP

1. Calibrate a microscope for FRAP according to the manufacturer's instruction. We have used a spinning disk confocal microscope UltraView ERS or Ultra-VIEW VoX CSUX1 system (PerkinElmer)(see above, 3.1).
2. Place the glass slide on a microscope. Use 100× objective lens with immersion oil.
3. Focus on yeast cells and place them in the center of the imaging field.

   Note: Positioning cells in the center of the imaging field minimizes variation.
4. Setting the imaging conditions. Use 2×2 binning for clearer fluorescence imaging if necessary. Selecting a single Z stack (the middle slice), which helps to minimize photo-bleaching from capturing multiple Z stacks and also minimize time intervals for fast time-lapse imaging. Time-interval can be as small as 1 sec for rapid image acquisition. If a cell cycle marker (such as Cdc3-GFP or Whi5-GFP, which we often use to examine cells in the M-G1 phase) is necessary to select cells at a specific cell cycle stage, set the acquisition set-up to capture an initial image with both fluorescent channels (such as GFP and RFP) and subsequent captures with RFP channel only in order to minimize unnecessary photobleaching.
5. Exposure time and gain value can be adjusted. In general, 100–200 msec exposure time was used for imaging Gic2-PBD-RFP. To minimize photobleaching and phototoxicity, shorter exposure times should be used for subsequent time-lapse imaging. Bleaching laser power and cycle can be selected according to the size of ROIs and the method optimized for each microscope system.
6. Select ROIs by drawing a shape of rectangle covering a part of Gic2-PBD-RFP within the fluorescent cap. Remember to record the exact size of ROIs and save ROIs for later data analysis.
7. Start the imaging acquisition including the initial bleaching point.

   Notes: Bleaching often occurs even beyond the selected ROIs, thus bleaching power and time need to be empirically determined for optimization. It is desirable to bleach more than 50% of the original fluorescence signal. Depending on the context of experiments, all conditions need to be optimized including laser intensity, numbers of laser pulse, size of ROIs, etc. In order to minimize phototoxicity, higher numbers of laser pulses with a lower laser power in a smaller ROI will be desirable.

Author Manuscript Author Manuscript Author Manuscript Author Manuscript

3.4 Methods forAnalyzingCdc42 activation dynamics

A threshold method for detecting and quantifying dynamic Cdc42-GTP cluster

Cdc42 activity changes both spatially and temporally during the cell cycle, which makes the detection and quantification of its local activation challenging. We have developed a "threshold method" to define a Cdc42-GTP cluster objectively using a simple statistical calculation. The specific steps are as follows. Examples of using the threshold method are described in section 4.

1. We use the image analysis software, Fiji/ImageJ (Schindelin, Arganda-Carreras, Frise, Kaynig, Longair, Pietzsch et al. 2012), to import the image data obtained by multi-dimensional time-lapse imaging experiment(s).
2. Use a 2D projection method (average projection or sum projection) to make a time-series image sequence.
3. Set the cell outline according to cytoplasmic fluorescence signal of a bright field image (if available).
4. Apply a custom-made Fiji/ImageJ macro (available on request)(Okada et al. 2013) to define the Cdc42-GTP cluster. In this macro, the average value and standard deviation of the fluorescence intensity of the pixels inside the cell outline are calculated. If a pixel has fluorescence intensity higher than a value of the average +2 standard deviations, the pixel is defined to be included in a Cdc42-GTP local cluster. For quantitative analysis, the total intensities of the pixels selected by this method is used (Fig. 3a).
5. The capability of the threshold method to detect a Cdc42-GTP cluster was validated (Fig. 3b). Wild-type haploid cells harboring Gic2-PBD-RFP and Cdc3-GFP (septin marker) grown to exponential phase were imaged by dual-color confocal microscopy. The depicted images were averaged projections of 11 z-slices with 0.6-μm spacing. The pixels calculated as part of a Cdc42-GTP cluster are shown in red. The cell outlines are highlighted in yellow.
6. Measure the average intensity of a region devoid of cells over time as the background signal.
7. Plot the sum of the intensities of the local cluster of Gic2-PBD-RFP after background subtraction and normalization (the peak value before bud emergence set as 100%) over time.

FRAP analysis

1. Import image sequences with ROIs and without ROIs as tiff files in Image J (NIH). Download ImageJ plugin to open image sequences if necessary. Use 16bit images for analysis.
2. Synchronize all opened windows and draw appropriate shapes along the ROIs in images. For accurate measurement, make sure that the actual bleaching area remains within a ROI shape in the time-lapse series. If cells moved during

Author Manuscript Author Manuscript Author Manuscript Author Manuscript

imaging acquisition, time-series images can be aligned using image J Plugins such as align stacks, image stabilizer and others.

3. Use appropriate FRAP template designed with proper formula for analysis. Obtain the total fluorescence intensity from the bleached area (ROIs) by drawing the same size ROIs over images. Subtract background by drawing a shape covering background area devoid of cells. For photobleaching correction, total intensities from the area of unbleached cells can be measured over time. Fluorescence changes should be plotted over time after background subtraction and photobleaching correction using Excel or other statistical programs such as GraphPad or Origin.

4. Draw a recovery graph by normalizing the prebleach intensity set to 100% and the intensity right after bleaching set to 0%. For curve fit line, you can use the exponential formula y=m1+m2*exp(−m3*x) for the curve fit of fluorescence recovery, in which m^3 is the off-rate (KaleidaGraph; Synergy Software). The half-time of fluorescence recovery was calculated as $t_{1/2} = \ln 2/m_3$ as previously described (Coffman et al., 2011).

As examples of FRAP experiments using Gic2-PBD-RFP, we describe here the dynamic behavior of Cdc42-GTP polarization during cell cycle in diploid cells. First, the Gic2-PBD polar cap was monitored by live-cell imaging in different stages of the cell cycle. To distinguish cells before and after cytokinesis, we used Cdc3-GFP: a group of cells with a large bud and a single septin ring (‘hourglass‘)(right before cytokinesis); and another group of cells with the septin double ring (from the onset of cytokinesis). Once the group of cells was selected based on the bud size and septin ring, a small region in the middle of Gic2-PBD-RFP cap was photo-bleached and fluorescence recovery was monitored by time-lapse imaging. Figure 2 shows an example of FRAP images obtained from unbudded cells. Gic2-PBD-RFP signal recovered right after the bleaching, thus we measured the recovery of fluorescence signals and plotted the recovery graph over time (Fig. 2b).

4. APPLICATION OF THE CDC42 BIOSENSOR

4.1 Dynamics of Cdc42 polarization in the G1 phase

The Cdc42 biosensor Gic2-PBD-RFP was used to examine Cdc42-GTP polarization dynamics by 3D time-lapse microscopy. In addition to the Gic2-PBD-RFP, we co-expressed either Cdc3-GFP as a marker for the bud neck and cell cycle progression, or Whi5-GFP as a cell cycle marker (Kang et al. 2014). The Cdc3-GFP ring splits into two rings at the onset of cytokinesis, and Cdc3-GFP appears at the presumptive bud site in the next G1 phase prior to disappearance of the old Cdc3-GFP ring. Whi5 enters the nucleus late in mitosis and exits the nucleus in mid G1, partitioning G1 phase into T_1 and T_2 (Di Talia, Skotheim, Bean, Siggia & Cross 2007). From a series of two-color live cell images and quantitative measurement of the Cdc42-GTP cluster by a threshold method as described above (3.4), we found stepwise activation of Cdc42 in G1 phase (see Fig. 4; Kang et al. 2014). These two steps of Cdc42 activation were observed in T_1 and T_2 and more distinctly separated in daughter cells, which have a longer G1 phase, than mother cells. Imaging cells at a lower temperature (such as 22°C) allowed more clear separation of the two steps than at 30°C

Author Manuscript Author Manuscript Author Manuscript Author Manuscript

because of slower growth. Using a *bud3* mutant that is defective in its GEF activity (*bud3ΔCR2*) and a *cdc24*^{ts} mutant, we showed that Cdc42 activation in the first and second step depends on Bud3 and Cdc24, respectively (see Fig. 4b). Time-lapse imaging of *cdc24*^{ts} cells also indicated that the first Cdc42-GTP peak appeared transiently in early G1 (i.e., prior to arrest in late G1) even after the temperature upshift to 37°C (Kang et al. 2014).

In another recent study, we used this Cdc42 biosensor to examine how a single, proper growth site was determined in haploid **a** or α cells. We imaged Gic2-PBD-RFPand Cdc3-GFP at 1min-time intervals at 22°C. The highest Cdc42-GTP peak appeared at multiple positions near the septin ring in daughter cells until the Cdc42-GTP polar cap became stable at the boundary of T_1 and T_2 (*i.e.*, right before the new septin clouds appear at the new bud site) (Fig. 4; See details in Lee et al., 2015). Thus, the Cdc42 biosensor represents a powerful method for uncovering novel Cdc42 activation dynamics and mechanisms underlying cell polarization.

4.2 Local inhibition of Cdc42 during septin ring formation

To investigate the spatial and temporal relationship between Cdc42 activity and septin ring assembly during bud emergence, we used a combination of Gic2-PBD-RFP and Cdc3-GFP (Fig. 5, (Okada et al. 2013). The dynamic behaviors of both probes were monitored by 5D time-lapse live cell imaging, and the spatial and temporal changes of the Cdc42-GTP cluster were analyzed using the threshold method (described in section 3.4).

During bud emergence, Cdc42-GTP and septins displayed distinct localization dynamics (Fig. 5, a and b) (Okada et al. 2013). Cdc42-GTP signal increased gradually and reached a peak as a bright cluster at the presumptive bud site 10–12 minutes before bud emergence. From the peak time of the cluster intensity to bud emergence, the signals of Cdc42-GTP and septins at the new bud site were inversely correlated. As the septin signal increased, the cluster intensity of Cdc42-GTP decreased. After bud emergence, septin accumulation continued at a slower rate, while a new Cdc42-GTP cluster formed at the bud cortex and intensified over time.

The inverse relationship between Cdc42-GTP and septins during bud emergence suggests that the newly recruited septins might constitute a negative feedback mechanism to inactivate Cdc42 at the presumptive bud site so that Cdc42 can be re-activated within the bud to drive exclusive cell growth within that compartment (Okada et al. 2013). To test this hypothesis, we performed time-lapse imaging of a temperature-sensitive septin mutant *cdc12-6* strain at the non-permissive temperature. Even at 39°C (the non-permissive temperature for the *cdc12-6* cells under our imaging conditions), the isogenic wild-type cells showed the normal Cdc42 inactivation-reactivation dynamics (Fig. 5d). In contrast, the *cdc12-6* septin mutant cells failed to display the transient inactivation of Cdc42 during bud emergence (Fig. 5, c and d). The cluster intensity of Cdc42-GTP increased continuously during bud emergence. As expected, septin accumulation at the presumptive bud site was not observed in the *cdc12-6* mutant at the non-permissive temperature. Consequently, the bud became elongated instead of ovoid in shape. This result not only provides strong support for our hypothesis but also illustrates the power of the biosensor in uncovering an unexpected

Author Manuscript Author Manuscript Author Manuscript Author Manuscript

interplay between Cdc42 activity and septin ring assembly during bud formation or polarized cell growth.

5. Concluding Remarks

Small GTPases are cellular switches that play vital roles in diverse processes such as cell polarization, cell migration, membrane trafficking, and cytokinesis (Etienne-Manneville 2004; Park & Bi 2007). Their activation and inactivation are exquisitely controlled to ensure that specific cellular events occur only at specific time and place. This also explains why there are far more GEFs and GAPs (GTPase-activating proteins) than their target GTPases (e.g. there are ~70 GEFs and 70 GAPs for 17 Rho GTPases in human genome) (Bernards 2003; Bernards & Settleman 2004). Small GTPases also share two key features in executing specific cellular functions – displaying a unique pattern of individual activation dynamics (e.g. Cdc42) and requiring spatiotemporal coordination with other GTPases (Rac, Rho, Rab, etc.). As we have demonstrated here, the biosensor for Cdc42-GTP in budding yeast has led to the discoveries of new activation and feedback mechanisms during polarization and bud morphogenesis. Strikingly, Cdc42 is inhibited while Rho1 is active during cytokinesis in budding yeast (Tong et al. 2007; Atkins, Yoshida, Saito, Wu, Lew & Pellman 2013; Okada et al. 2013; Onishi, Ko, Nishihama & Pringle 2013; Okada, Wloka & Bi 2017). Thus, it will be critically important to explore the potential mutual antagonism between Cdc42 and Rho1 during cytokinesis (Atkins et al. 2013; Onishi et al. 2013). A similar relationship between the GTPases has also been suggested for the budding process (Gao, Caviston, Tcheperegine & Bi 2004). Such studies require the development of a rigorously tested biosensor for Rho1 in budding yeast, which has yet to be done. In mammalian cells, the activities of small GTPases such as Ras, Rho, Cdc42, and Rac are coordinately regulated, often displaying mutual antagonism in processes such as cell migration (Nobes & Hall 1999; Tsubouchi, Sakakura, Yagi, Mazaki, Schaefer, Yano et al. 2002; Machacek, Hodgson, Welch, Elliott, Pertz, Nalbant et al. 2009), cell-cell adhesion (Arthur, Noren & Burridge 2002; Bruewer, Hopkins, Hobert, Nusrat & Madara 2004), and chemotaxis (Xu, Wang, Van Keymeulen, Herzmark, Straight, Kelly et al. 2003). Biosensors for different small GTPases have played a key role in defining their spatiotemporal relationships in a specific process. These biosensors and newly developed ones will continue to be instrumental for understanding the functions and mechanisms of individual GTPases, discovering their new roles, and understanding their coordination with other GTPases in a given process.

Acknowledgments

We thank the members of Bi and Park laboratories for discussions, Dr. Pil Jung Kang for providing the PBD-binding figure, Dr. Andrea Stout at the CDB imaging Core, and members of Dr. Jian-Qiu Wu's lab for technical advice. This work is supported by the National Institutes of Health grants GM115420 (to E.B.) and R01 GM114582 (to H.-O.P.).

Abbreviations

GTPase	guanosine triphosphatase
CRIB	Cdc42- and Rac-interactive binding

Author Manuscript Author Manuscript Author Manuscript Author Manuscript

PBD	p21-binding domain
FRAP	fluorescence recovery after photobleaching
FRET	fluorescence resonance energy transfer
GEF	Guanine nucleotide exchange factor
GFP	green fluorescent protein
PAK	p21-activated kinase

References

Arthur WT, Noren NK, Burridge K. Regulation of Rho family GTPases by cell-cell and cell-matrix adhesion. Biol Res. 2002; 35:239–246. [PubMed: 12415742]

Atkins BD, Yoshida S, Saito K, Wu CF, Lew DJ, Pellman D. Inhibition of Cdc42 during mitotic exit is required for cytokinesis. J Cell Biol. 2013; 202:231–240. [PubMed: 23878274]

Bendezu FO, Vincenzetti V, Vavylonis D, Wyss R, Vogel H, Martin SG. Spontaneous Cdc42 polarization independent of GDI-mediated extraction and actin-based trafficking. PLoS Biol. 2015; 13:e1002097. [PubMed: 25837586]

Bernards A. GAPs galore! A survey of putative Ras superfamily GTPase activating proteins in man and Drosophila. Biochim Biophys Acta. 2003; 1603:47–82. [PubMed: 12618308]

Bernards A, Settleman J. GAP control: regulating the regulators of small GTPases. Trends Cell Biol. 2004; 14:377–385. [PubMed: 15246431]

Bruewer M, Hopkins AM, Hobert ME, Nusrat A, Madara JL. RhoA, Rac1, and Cdc42 exert distinct effects on epithelial barrier via selective structural and biochemical modulation of junctional proteins and F-actin. Am J Physiol Cell Physiol. 2004; 287:C327–C335. [PubMed: 15044152]

Coffman VC, Wu P, Parthun MR, Wu JQ. CENP-A exceeds microtubule attachment sites in centromere clusters of both budding and fission yeast. The Journal of Cell Biology. 2011; 195:563–572. [PubMed: 22084306]

Di Talia S, Skotheim JM, Bean JM, Siggia ED, Cross FR. The effects of molecular noise and size control on variability in the budding yeast cell cycle. Nature. 2007; 448:947–951. [PubMed: 17713537]

Etienne-Manneville S. Cdc42 - the centre of polarity. J. Cell Sci. 2004; 117:1291–1300. [PubMed: 15020669]

Gao XD, Caviston JP, Tcheperegine SE, Bi E. Pxl1p, a paxillin-like protein in Saccharomyces cerevisiae, may coordinate Cdc42p and Rho1p functions during polarized growth. Mol Biol Cell. 2004; 15:3977–3985. [PubMed: 15215315]

Jaquenoud M, Peter M. Gic2p may link activated Cdc42p to components involved in actin polarization, including Bni1p and Bud6p (Aip3p). Mol. Cell. Biol. 2000; 20:6244–6258. [PubMed: 10938101]

Kang PJ, Lee ME, Park HO. Bud3 activates Cdc42 to establish a proper growth site in budding yeast. J Cell Biol. 2014; 206:19–28. [PubMed: 25002677]

Lee ME, Lo WC, Miller KE, Chou CS, Park HO. Regulation of Cdc42 polarization by the Rsr1 GTPase and Rga1, a Cdc42 GTPase-activating protein, in budding yeast. J Cell Sci. 2015; 128:2106–2117. [PubMed: 25908844]

Lo WC, Lee ME, Narayan M, Chou CS, Park HO. Polarization of diploid daughter cells directed by spatial cues and GTP hydrolysis of Cdc42 budding yeast. PLoS One. 2013; 8:e56665. [PubMed: 23437206]

Machacek M, Hodgson L, Welch C, Elliott H, Pertz O, Nalbant P, et al. Coordination of Rho GTPase activities during cell protrusion. Nature. 2009; 461:99–103. [PubMed: 19693013]

Nalbant P, Hodgson L, Kraynov V, Toutchkine A, Hahn KM. Activation of endogenous Cdc42 visualized in living cells. Science. 2004; 305:1615–1619. [PubMed: 15361624]

Author Manuscript Author Manuscript Author Manuscript Author Manuscript

Nobes CD, Hall A. Rho GTPases control polarity, protrusion, and adhesion during cell movement. J Cell Biol. 1999; 144:1235–1244. [PubMed: 10087266]

Okada S, Leda M, Hanna J, Savage NS, Bi E, Goryachev AB. Daughter cell identity emerges from the interplay of Cdc42, septins, and exocytosis. Dev Cell. 2013; 26:148–161. [PubMed: 23906065]

Okada S, Wloka C, Bi E. Analysis of protein dynamics during cytokinesis in budding yeast. Methods Cell Biol. 2017 In press.

Onishi M, Ko N, Nishihama R, Pringle JR. Distinct roles of Rho1, Cdc42, and Cyk3 in septum formation and abscission during yeast cytokinesis. J Cell Biol. 2013; 202:311–329. [PubMed: 23878277]

Ozbudak EM, Becskei A, van Oudenaarden A. A system of counteracting feedback loops regulates Cdc42p activity during spontaneous cell polarization. Dev. Cell. 2005; 9:565–571. [PubMed: 16198298]

Park H-O, Bi E. Central roles of small GTPases in the development of cell polarity in yeast and beyond. Microbiol. Mol. Biol. Rev. 2007; 71:48–96. [PubMed: 17347519]

Pertz O, Hodgson L, Klemke RL, Hahn KM. Spatiotemporal dynamics of RhoA activity in migrating cells. Nature. 2006; 440:1069–1072. [PubMed: 16547516]

Schindelin J, Arganda-Carreras I, Frise E, Kaynig V, Longair M, Pietzsch T, et al. Fiji: an open-source platform for biological-image analysis. Nat Methods. 2012; 9:676–682. [PubMed: 22743772]

Smith SE, Rubinstein B, Mendes Pinto I, Slaughter BD, Unruh JR, Li R. Independence of symmetry breaking on Bem1-mediated autocatalytic activation of Cdc42. J Cell Biol. 2013; 202:1091–1106. [PubMed: 24062340]

Tong Z, Gao X-D, Howell AS, Bose I, Lew DJ, Bi E. Adjacent positioning of cellular structures enabled by a Cdc42 GTPase-activating protein mediated zone of inhibition. J. Cell Biol. 2007; 179:1375–1384. [PubMed: 18166650]

Tsubouchi A, Sakakura J, Yagi R, Mazaki Y, Schaefer E, Yano H, et al. Localized suppression of RhoA activity by Tyr31/118-phosphorylated paxillin in cell adhesion and migration. J Cell Biol. 2002; 159:673–683. [PubMed: 12446743]

Wedlich-Soldner R, Wai SC, Schmidt T, Li R. Robust cell polarity is a dynamic state established by coupling transport and GTPase signaling. J. Cell Biol. 2004; 166:889–900. [PubMed: 15353546]

Xu J, Wang F, Van Keymeulen A, Herzmark P, Straight AF, Kelly K, et al. Divergent signals and cytoskeletal assemblies regulate self-organizing polarity in neutrophils. Cell. 2003; 114:201–214. [PubMed: 12887922]

Author Manuscript Author Manuscript Author Manuscript Author Manuscript

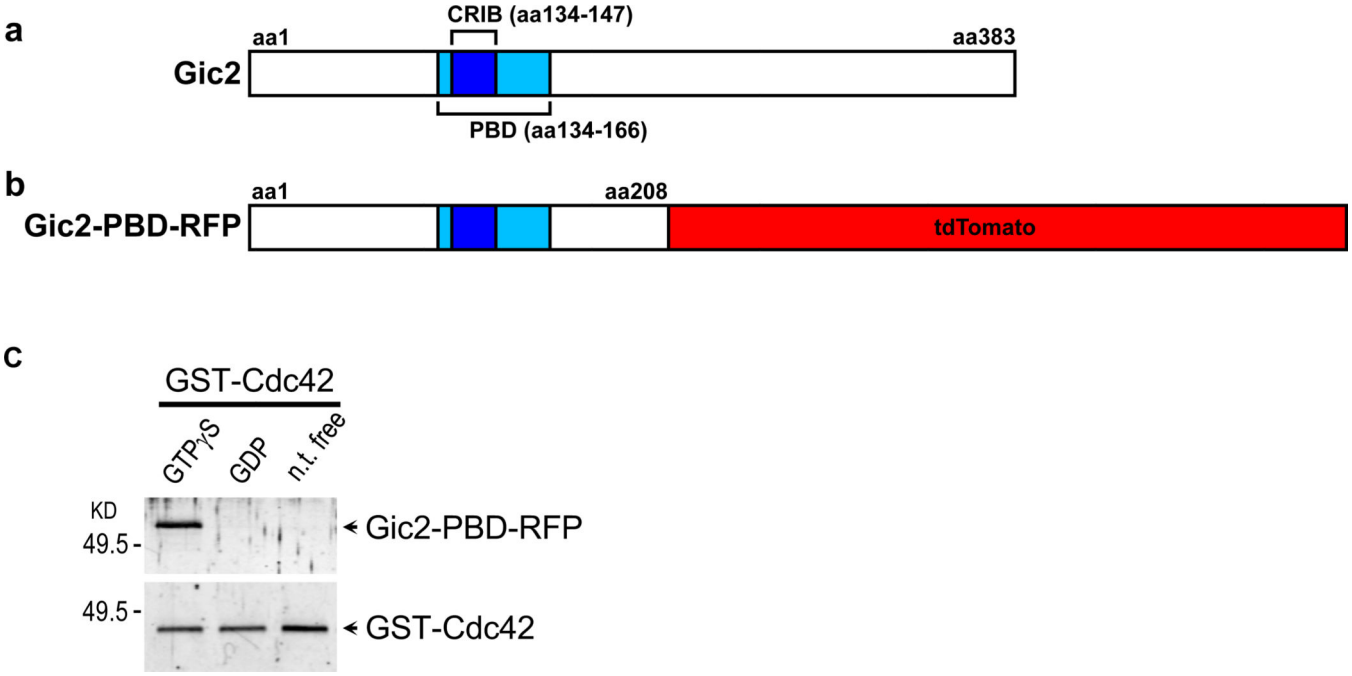

Figure 1. Schematic representation of Gic2 and Gic2-PBD-RFP and association of PBD-RFP with Cdc42-GTP

(a) Domain structure of Gic2-PBD (p21-binding domain, aa133–166) is shown in cyan, and CRIB (Cdc42/Rac-interactive binding) domain is shown in blue.

(b) Domain structure of Gic2-PBD-RFP. A red fluorescent protein tdTomato fused to the N-terminal portion of Gic2 is shown in red.

(c) Association of Gic2-PBD-RFP with GTP-bound Cdc42. GST-Cdc42 purified from the insect cells was immobilized on glutathione Sepharose beads, loaded with GTPγS or GDP, or stripped with EDTA to deplete nucleotides bound to Cdc42 (n.t. free), and then incubated with yeast extracts containing Gic2-PBD-RFP. Gic2-PBD-RFP was detected with polyclonal antibodies against RFP (upper panel); GST-Cdc42 was detected with polyclonal antibodies against GST (lower panel) (Data provided by Dr. P. J. Kang).

Author Manuscript Author Manuscript Author Manuscript Author Manuscript

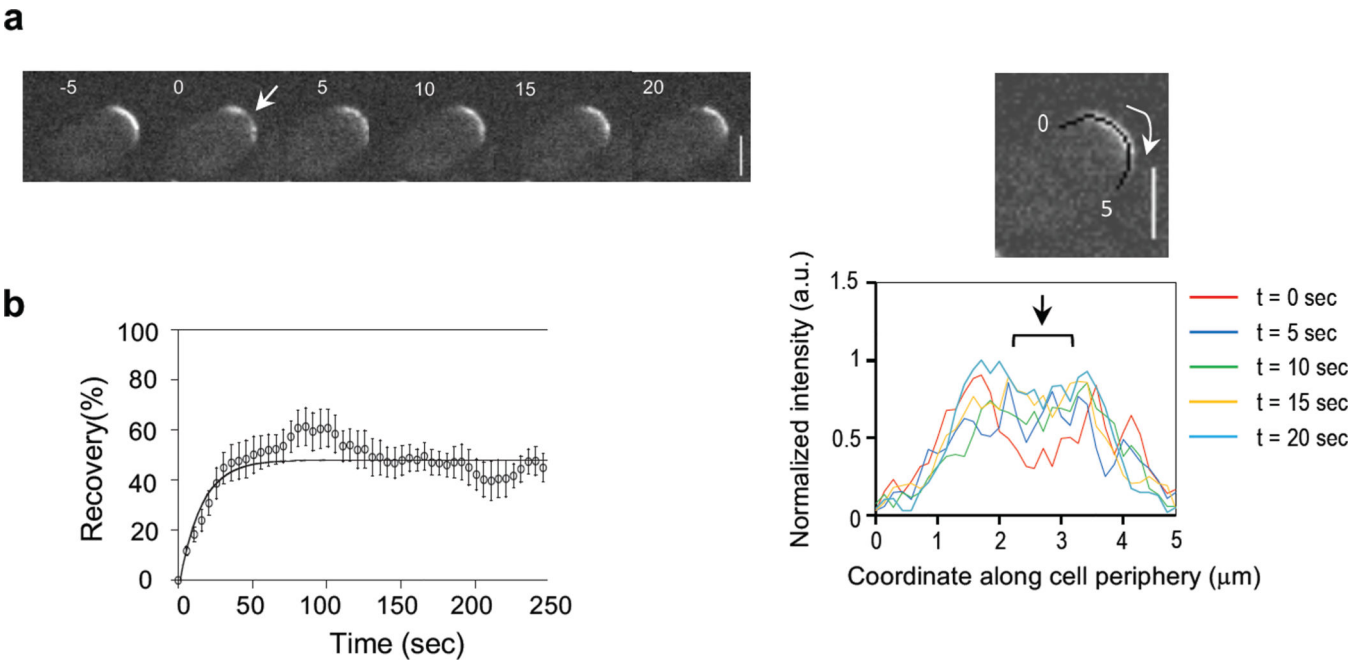

Figure 2. Gic2-PBD-RFP is highly dynamic

(a) Intensity profile of PBD-RFP cluster along the periphery of **a**/α cell in the G1 phase after bleaching. Numbers indicate time (in sec) relative to the bleaching (t=0). Bleached region is marked with a white arrow on the image and a black arrow with bracket on the graph. Each colored line in the graph represents a different time point. Scale bar, 3μm

(b) FRAP analysis of PBD-RFP cluster in G1 (n = 10 cells). Relative intensity is normalized to the pre-bleach intensity. Mean ± SEM. The curve fit line is drawn in black-colored line.

Author Manuscript Author Manuscript Author Manuscript Author Manuscript

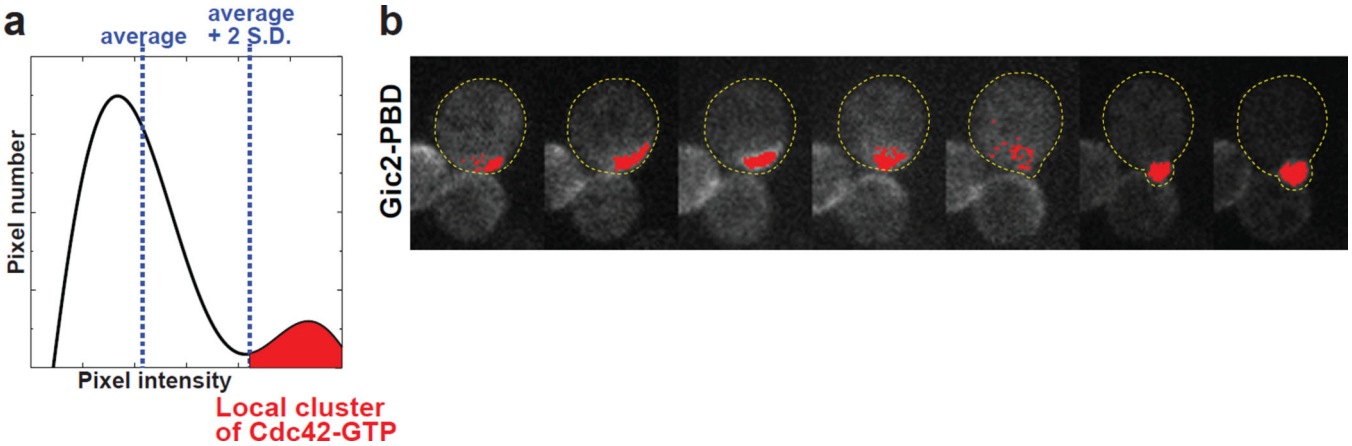

Figure 3. The threshold method for quantifying Cdc42-GTP signal in live cells

(a) Using the threshold method to assign pixels to a cluster of Cdc42-GTP. After the measurement of the intensities of all pixels inside the cell outline, if a pixel has an intensity higher than the value of the average + 2 standard deviations, the pixel is assigned to a cluster of Cdc42-GTP.

(b) An example of defining a Cdc42-GTP cluster by the threshold method. Gic2-PBD-RFP signal is shown in grayscale. The pixels calculated as a part of the Cdc42-GTP local cluster are shown in red. The cell outlines are marked in yellow. (Adapted from Okada et al., 2013)

Author Manuscript Author Manuscript Author Manuscript Author Manuscript

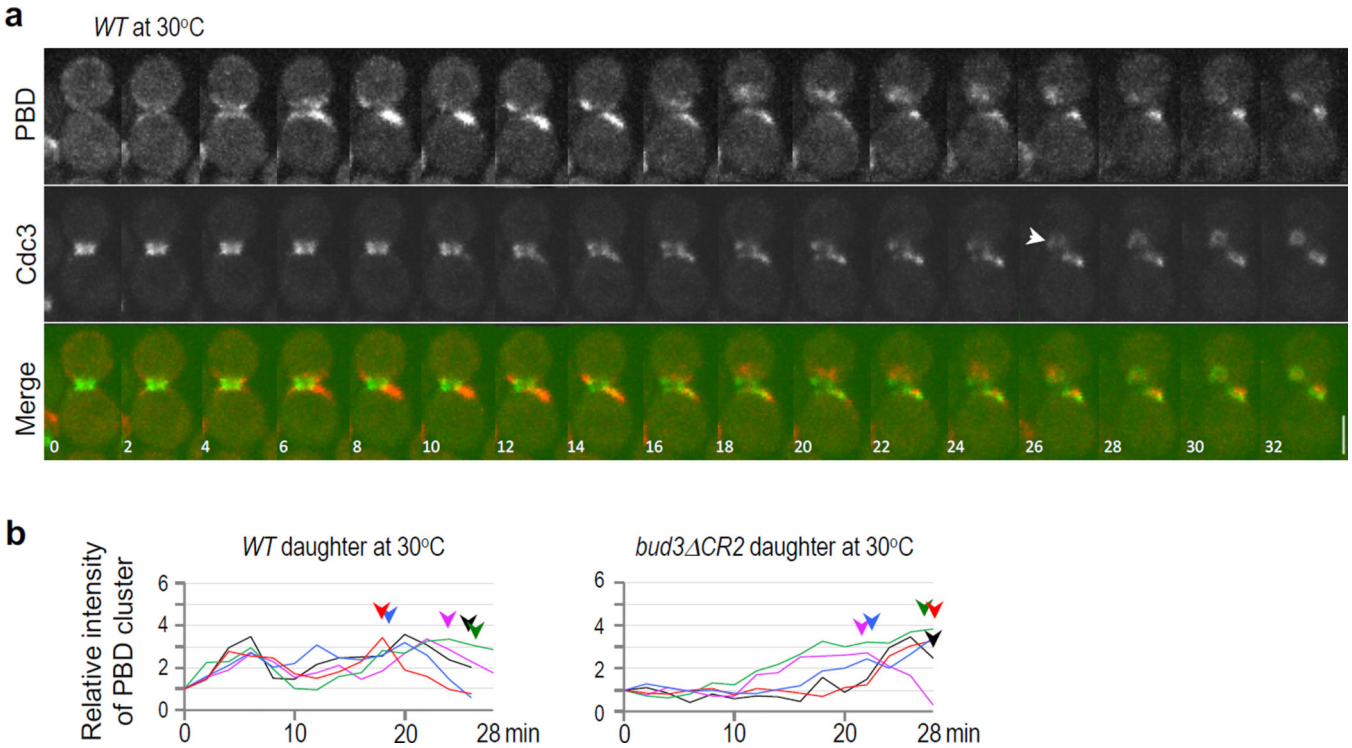

Figure 4. Dynamic Cdc42-GTP polarization during selection of a new bud site

(a) Time-lapse imaging of PBD-RFP and Cdc3-GFP in wild-type cells at 30°C. Arrowheads mark the first appearance of a new septin in a daughter cell. Numbers indicate time (in minutes) from the onset of cytokinesis (t = 0). Scale bar, 3 μm. Adapted from Kang, P. J., Lee, M. E., Park, H.-O. (2014) Bud3 activates Cdc42 to establish a proper growth site in budding yeast. The Journal of Cell Biology, 206, 19-28. doi: 10.1083/jcb.201402040

(b) PBD-RFP intensity is compared in daughter cells of wild-type and *bud3ΔCR2* cells at 30°C. PBD-RFP intensity was normalized to intensity at the onset of cytokinesis (t = 0). Each colored arrowhead marks the time point when new septin clouds were first visible (or estimated) in each daughter cell for each corresponding colored line. ©Kang et al., 2014. Originally published in Journal of Cell Biology. doi: 10.1083/jcb.201402040

Author Manuscript Author Manuscript Author Manuscript Author Manuscript

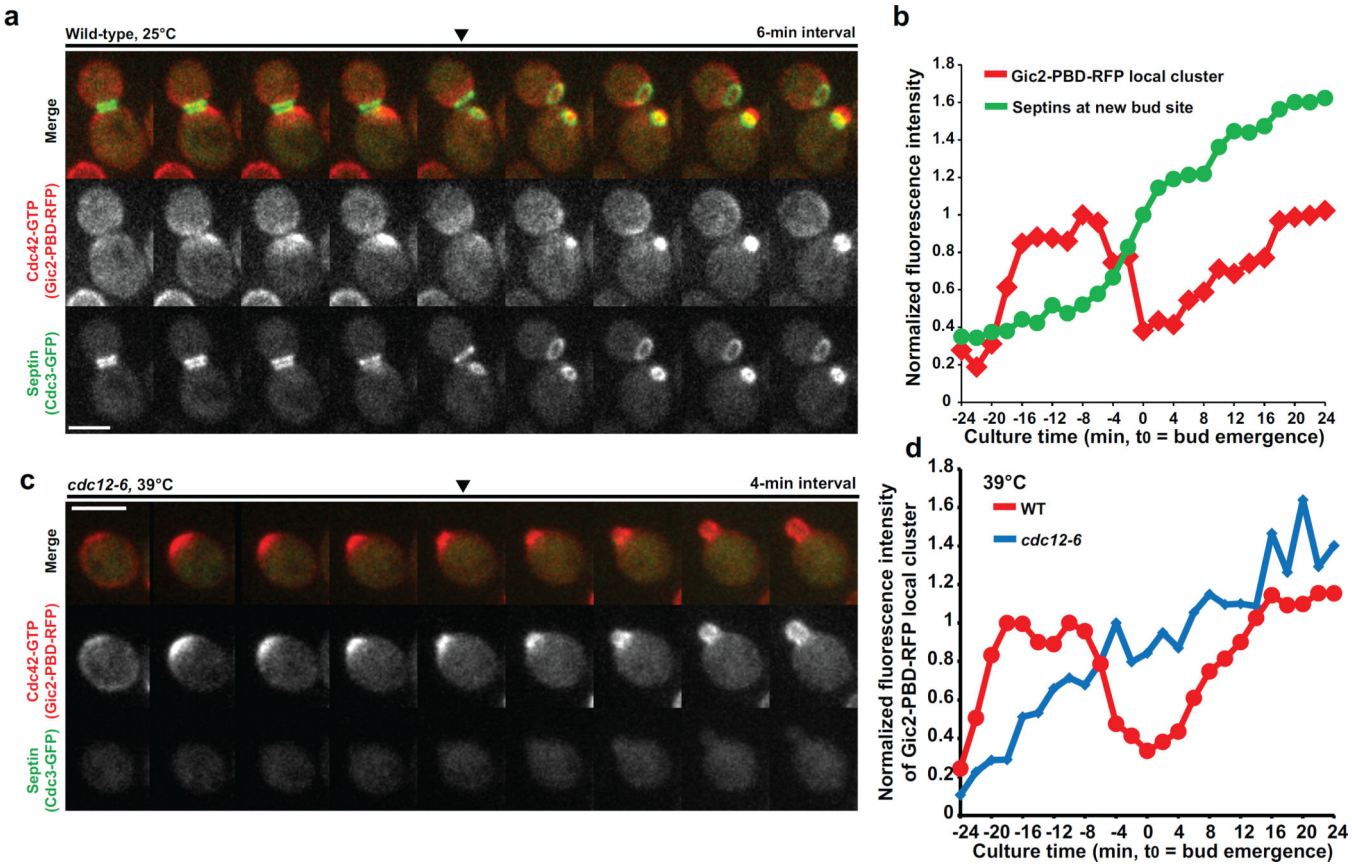

Figure 5. Local inhibition of Cdc42 during septin ring formation

(a) An image sequence showing the dynamic behavior of Cdc42-GTP (Gic2-PBD-RFP, red) and septins (Cdc3-GFP, green) during bud emergence. The image sequence was generated by average projection of 11 z-slices with 0.6 μm spacing. Filled triangle indicates the timing of bud emergence. Scale bar, 3 μm.

(b) Quantitative analysis of Cdc42-GTP cluster and septin accumulation at the site of polarization during bud emergence. The cell shown in (a) was used for the analysis. Normalized total intensity of Cdc42-GTP cluster is shown in red, and the normalized septin intensity at new bud site is shown in green.

(c) Polarized growth of septin mutant *cdc12-6* strain. At the non-permissive temperature (39°C), intensity of the Cdc42-GTP cluster does not show a transient decrease around bud emergence. Scale bar, 3 μm.

(d) Quantitative analysis of Cdc42-GTP cluster during bud emergence in *cdc12-6* mutant and isogenic wild-type cells cultured at 39°C. The temporal changes of the normalized total intensity of Cdc42-GTP cluster in wild-type and *cdc12-6* mutant cells are shown in red and blue, respectively.